Examining the rheology of 9-octylheptadecane to giga-pascal pressures

Clare McCabe[a] and Shengting Cui
Department of Chemical Engineering, University of Tennessee, Knoxville, Tennessee 37996-2200 and Chemical Technology Division, Oak Ridge National Laboratory, Oak Ridge, Tennessee 37831-6181

Peter T. Cummings
Departments of Chemical Engineering, Chemistry and Computer Science, University of Tennessee, Knoxville, Tennessee 37996-2200 and Chemical Technology Division, Oak Ridge National Laboratory, Oak Ridge, Tennessee 37831-6181

Peter A. Gordon and Roland B. Saeger
Corporate Strategic Research Centre, ExxonMobil Research and Engineering Company, Annandale, New Jersey 08801

(Received 18 August 2000; accepted 31 October 2000)

The properties of alkanes in the $C_{20}-C_{40}$ mass range are of fundamental importance in industrial applications as they are important constituents of synthetic lubricant base stocks. In an extension to earlier work on alkanes in the $C_{20}-C_{40}$ carbon number range we present the results of molecular simulations for 9-octylheptadecane, a starlike isomer of C_{25}. Both equilibrium (EMD) and nonequilibrium molecular dynamics (NEMD) simulations have been performed under ambient state conditions and to pressures in the gigapascal range. The EMD simulations focus on calculations of the rotational relaxation times, while the NEMD simulations reveal the dependence of the viscosity on strain rate. Additionally, we calculate the viscosity number and pressure–viscosity coefficient for 9-octylheptadecane and compare the results with those obtained experimentally. © *2001 American Institute of Physics.* [DOI: 10.1063/1.1334676]

INTRODUCTION

An understanding of the rheological properties of lubricant components in vital to the petrochemical industry. In particular, the properties of alkanes in the $C_{20}-C_{40}$ mass range are of fundamental importance in industrial applications as they are important constituents of synthetic lubricant base-stocks. Given the wide range of operating conditions lubricants are subjected to in practical applications a consideration of not only the viscosity, but also the viscosity–temperature and viscosity–pressure behavior is vital to determine if a substance would make a good lubricant component.

The need to characterize the influence of temperature on lubricant performance has been recognized for a long time. In 1929 the kinematic viscosity index (VI)[1] was introduced as a means to do exactly that, though since its introduction numerous definitions for the VI have been proposed as lubricant performance has improved. Currently the VI is determined using the ASTM standard method (D2270-93), in which the kinematic viscosity of the test substance at 40 °C and 100 °C is compared against that of two reference oils. Generally the higher the VI the less the substance is affected by temperature, and therefore the better the potential lubricant. Although the VI is widely used and accepted as a measure of lubricant performance, it suffers from the major drawback that it is undefined for lubricants with a kinematic viscosity less than 2cSt at 100 °C. The viscosity number (VN) was recently proposed[2] as an alternative measure of lubricant performance. It is applicable over a wider range of temperatures and has been shown to correlate well with the VI. Calculation of the VN of the test substance is trivial given the kinematic viscosity at 40 °C and 100 °C. In a similar manner to the calculation of the VI the kinematic viscosity at these two temperatures is substituted into the Walther equation,

$$\log\log(\nu+0.7)=A+B\log T, \tag{1}$$

where ν is the kinematic viscosity in cSt and T the temperature in Kelvin. Once the coefficient B has been determined from Eq. (1), the VN can be easily obtained using

$$\mathrm{VN}=\left(1+\frac{3.55+B}{3.55}\right)\times 100. \tag{2}$$

Like the VI, the larger the VN the smaller the change in viscosity with temperature, and hence the ''better'' the test substance should perform as a lubricant. However, we note that while the VI or VN provides a good guide to lubricant behavior with temperature it is not the only relevant property. For example, linear alkanes have a high VI, but because of their high melting points, they have a high pour point and are therefore not useful as lubricants in most practical applications since they are solids at ambient conditions.

Although viscosity is a function of both temperature and pressure, the effect on the viscosity of a small change in pressure from atmospheric is quite small compared with temperature. For that reason much less effort has been devoted to examining the influence of pressure. However, the performance of machine elements such as gears and roller bearings depends on lubricants that routinely are subjected to pres-

[a]Corresponding author. Electronic mail: CLARE@UTK.EDU

sures in the GPa range. Relative to atmospheric conditions, these pressures can induce viscosity increases of several orders of magnitude. The pressure–viscosity coefficient, α, has been used to characterize the pressure dependence of the viscosity, though over the years it has been defined in a number of ways in the literature, the final choice usually depending on the application or the particular pressure–viscosity correlation chosen.[3] Perhaps the most common definition comes from the Barus relation,[4]

$$\eta(T,P) = \eta(T,0)\exp[\alpha(T)P], \tag{3}$$

where η is the viscosity and α the pressure–viscosity coefficient.

Unfortunately, in the literature there is very little experimental data available on the rheological properties of hydrocarbons in the mass range of interest, especially at high pressures. The most comprehensive experimental study of the viscosity of lubricants to high pressures was undertaken at Harvard University[5] in the late 1940s. They reported viscosity and density data for 40 lubricants, including pure hydrocarbons, mineral oils, and synthetic lubricants, to pressures of 1 GPa and temperatures up to 200 °C. Most of what we know about the rheological properties of hydrocarbons at atmospheric pressure comes from the American Petroleum Institute (API) research project 42,[6] a database on the physical properties of pure hydrocarbons completed in the late 1960s. Although API 42 contains data for some 273 molecules, less than a quarter are in the C_{20}–C_{40} mass range, which overall represents a infinitesimally small fraction of the total number of possible structural isomers.

In order to gain further insight into the relationship between molecular architecture and lubricant performance additional investigation into the properties of C_{20}–C_{40} alkanes is needed. With that goal in mind, given the cost and time involved in experimental synthesis and testing, computer simulation studies are becoming an increasingly attractive alternative. Furthermore, it is often difficult to accurately measure the temperature and pressure of lubricants in operation, but these variables can be set or measured unambiguously in a computer experiment. Molecular simulations examining rheological properties of industrially important molecules, such as the alkanes, were initially limited to short, mainly linear molecules (see, for example, Refs. 7–11). However, with the recent advances in computational power, and the development of more realistic models and suitable algorithms, it is now possible to perform simulations on molecules of real practical interest. In the early 1990s, Morris *et al.*[8] examined the rheology of *n*-decane and *n*-eicosane as a function of shear rate at a single state point using NEMD simulation. For both molecules using a constrained alkane model they observed a regime of shear thinning behavior followed by shear thickening at higher strain rates. The rheology of *n*-eicosane was later re-examined by Travis and Evans,[12] who questioned the influence of the thermostat used in the simulation on the predicted rheological behavior. Around this time a number of molecular dynamics simulation studies on the rheology of alkanes were reported in the literature. In the mass range of interest, Cui *et al.*[13] examined *n*-tetracosane, 10-n-hexylnonadecane, and squalane; Mundy and co-workers[14] studied *n*-triacontane and squalane; and Khare *et al.*[15] investigated *n*-docosane, *n*-octacosane, and 5,12-dipropylhexadecane. These studies all compared the strain rate dependent viscosities of both linear and branched molecules at a single temperature using similar fully flexible models. The influence of temperature on the viscosity of a branched alkane was first investigated by Moore *et al.*,[16] who reported the shear rate dependent viscosity, and the calculation of the VI for squalane from NEMD simulations. This work represented the first accurate quantitative prediction of the VI by molecular simulation. An extensive study on the influence of a side chain and its position on the rheological properties of isomers of *n*-eicosane as a function of the shear rate and temperature was performed by Lahtela *et al.*[17] Using a constrained alkane model they showed that for the model eicosane isomers a branch significantly increased the viscosity compared to the *n*-alkane case, though the location of the branch had little noticeable effect. More recently, Kioupis and Maginn[18] have examined the rheological properties of three isomers of C_{18} by EMD and NEMD simulation using the united atom transferable potentials for phase equilibria (TraPPE-UA) force field model. While they underpredicted the zero-shear viscosity, the VN for *n*-octadecane was accurately determined. A similar effect was seen by Moore and co-workers,[19] who examined the rheological behavior of isomers of C30 by molecular simulation. A calculation of the VI for 9-octyldocosane further supported the observation that, while these united atom models underpredict the actual experimental Newtonian viscosity, they can accurately determine the temperature dependence.

In this work we have undertaken EMD and NEMD simulations of 9-octylheptadecane at several state points, ranging from ambient conditions to high pressures in the gigapascal range. The NEMD simulations span a wide range of strain rates (10^{11}–$10^{7}\ s^{-1}$) from which we have determined the zero-shear, or Newtonian viscosity, VN and pressure–viscosity coefficient.

TABLE I. Lennard-Jones potential model parameters.

United atom	σ/Å	(ϵ/k_B)/K
CH_3	3.93	114
CH_2	3.93	47
CH	3.81	40

SIMULATION DETAILS

The model used to describe the alkane molecules is that of Siepmann *et al.*,[20,21] which was later extended to branched alkanes by Mondello and Grest.[22] As in earlier work[10] we use the modification of Mundy and co-workers[11] in which the fixed bond length is replaced by a stiff harmonic potential to generate a fully flexible model. We will briefly describe the model and the simulation methods. The reader is referred to the original papers for full details.

In this united atom description of the alkanes the methyl, methylene, and methyne groups are each modeled and individually treated as single spherical interaction sites with the

TABLE II. Torsional potential parameters.

	(a_0/k_B)/K	(a_1/k_B)/K	(a_2/k_B)/K	(a_3/k_B)/K
X–CH_2–CH_2–Y	1010	2019	136.4	−3165
X–CH–CH_2–Y	409.6	901.8	195.8	−1848

TABLE IV. Rotational relaxation times for 9-octylheptadecane estimated from EMD simulations.

State point	A	B	C	D	E
τ/ps	702	189	4334	7523	9852

interaction center located at the center of each carbon atom. A Lennard Jones potential describes the intermolecular interactions, and the intramolecular interactions between sites separated by three or more bonds. A cut-off distance of 9.85 Å ($2.5\sigma_{CH_2}$) was used. Details of the potential model size and energy parameters can be found in Table I. Simple Lorentz–Berthelot combining rules were used to determine the cross or unlike interactions. Bond stretching is described by a harmonic potential with an equilibrium bond distance of $r_{eq}=1.54$ Å and force constant $k_a/k_B=4\,529\,00$ K Å^{-2} (where k_B is Boltzmann's constant). The bond angle bending term is also described by a harmonic potential with an equilibrium angle of $\theta_{eq}=114°$ and force constant $k_b/k_B=62\,500$ Krad^{-2}. In the extension to branched alkanes by Mondello and Grest[22] and *ad hoc* harmonic potential similar to the bending term was introduced to prevent the unphysical umbrella inversion of the tertiary carbon atoms ($\theta=27.25°$ and $k_a/k_B=40\,258$ Krad^{-2}). Finally, torsional motion characterizing the preferred orientational and rotational barriers around all non-terminal bonds is described through the potential of Jorgensen, details of which can be found in Table II.

The alkanes were simulated under planar Couette flow using the SLLOD equations of motion with Lees–Edwards boundary conditions and a Nosé thermostat. The multiple time step technique from the work of Tuckerman *et al.*[23] extended to NEMD by Cui *et al.*[24] was used to integrate the equations of motion, all the intramolecular interactions were treated as fast motions, and the intermolecular interactions as the slow motion. For the fast mode motion a time step of 0.235 fs was used, and for the slow mode motion the time step was 2.35 fs. The simulations were performed with 100 molecules in a cubic box. To generate the starting configurations each atom was given a small LJ diameter and the molecules placed on a lattice in the all *trans* conformation, with the center of mass at the cubic lattice points. During this initial equilibration period the atoms are grown to full size and then allowed to equilibrate for a further 5000 ps. This equilibrium configuration provides the starting point for both the EMD and high strain rate NEMD simulations. At the lowest strain rates the final configuration of a higher strain rate was used for the starting configuration. The strain rate-dependent properties were calculated once the system has reached a steady state under the influence of shear flow. The strain rate-dependent viscosity was calculated using the usual Irving–Kirkwood expression for the pressure tensor.[25]

TABLE III. State points studied.

State point	Temperature/K	Pressure/GPa	Density/gcm^{-3}
A	310.93	1.01E-04	0.791
B	372.04	1.01E-04	0.751
C	372.04	0.682	0.943
D	372.04	0.829	0.964
E	372.04	0.958	0.980

RESULTS

We have simulated 9-octylheptadecane at a range of state points, full details of which are given in Table III. The influence of both temperature and pressure on the viscosity is investigated by considering state points at two different temperatures and a range of pressures.

In addition to the rheological properties of 9-octylheptadecane we are also interested in a number of equilibrium properties, such as the rotational relaxation time τ, which is a useful quantity when examining the transition from Newtonian to non-Newtonian behavior. When the shear field exceeds the inverse of the longest relaxation time the system cannot respond fast enough to the deformation due to the flow field and alignment of the molecules with the flow field begins to appear, resulting in reduced viscosity. Hence, the inverse of the rotational relaxation time provides a good guide to the transition from the Newtonian to the non-Newtonian regime. The rotational relaxation time for 9-octylheptadecane at all five state points was calculated from the rate of exponential decay of the orientational relaxation of the longest principal axis of each molecule's ellipsoid of inertia, the results of which are given in Table IV. As would be expected, the molecules have a longer relaxation time at the lower temperature and higher densities studied

In Fig. 1 we present the strain rate dependent viscosity for 9-octylheptadecane under ambient conditions as a log–log plot (state points A and B in Table III). Details of the numerical data and run times can be found in Table V. In the

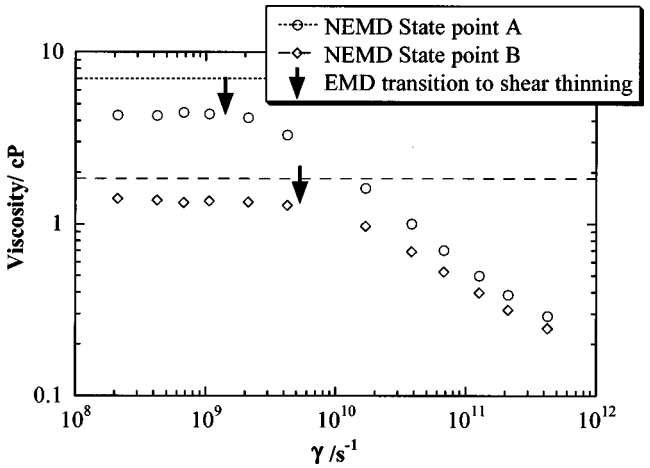

FIG. 1. Viscosity as a function of strain rate at state points A and B from Table III.

TABLE V. Viscosity versus strain rate data for 9-octylheptadecane at 311 and 372 K.

Strain rate/ s^{-1}	State point A		State point B	
	Run time/ns	Viscosity/cP	Run time/ns	Viscosity/cP
4.24×10^{11}	3.70	0.2909	4.10	0.2472
2.12×10^{11}	3.85	0.3861	3.23	0.3166
1.27×10^{11}	5.47	0.5011	3.35	0.3986
6.78×10^{10}	5.26	0.7054	4.15	0.5278
3.82×10^{10}	5.50	1.004	4.18	0.6918
1.70×10^{10}	9.20	1.617	7.92	0.9756
4.24×10^{9}	4.41	3.303	10.6	1.286
2.12×10^{9}	6.13	4.170	16.5	1.343
1.06×10^{9}	20.3	4.376	14.3	1.365
6.78×10^{8}	23.6	4.470	22.2	1.332
4.24×10^{8}	11.3	4.451	11.9	1.377
2.12×10^{8}	20.7	4.301	22.2	1.407

figure the horizontal lines correspond to the experimental zero shear viscosity for each state point[6] and the arrows are the inverse of the rotational relaxation times estimated from equilibrium simulations. We can see from the figure the viscosity shows shear-thinning behavior at high strain rates and a Newtonian plateau at the lowest strain rates. The onset of shear thinning as the strain rate increases occurs at higher strain rates for the higher temperature studied, which is consistent with earlier work. We also see from Fig. 1 the transition from Newtonian to non-Newtonian behavior predicted by the NEMD simulations correlates well with the inverse of the rotational relaxation time determined from the EMD simulations.

In Fig. 2 we present the strain rate dependent viscosity of 9-octylheptadecane at the remaining state points from Table III. Here we are interested in the pressure (or, equivalently, the density dependence) of the viscosity. Again, the horizontal lines correspond to the experimental zero shear viscosity[5] for each state point and the arrows are the inverse of the rotational relaxation times determined from the equilibrium simulations. Details of the numerical data and run

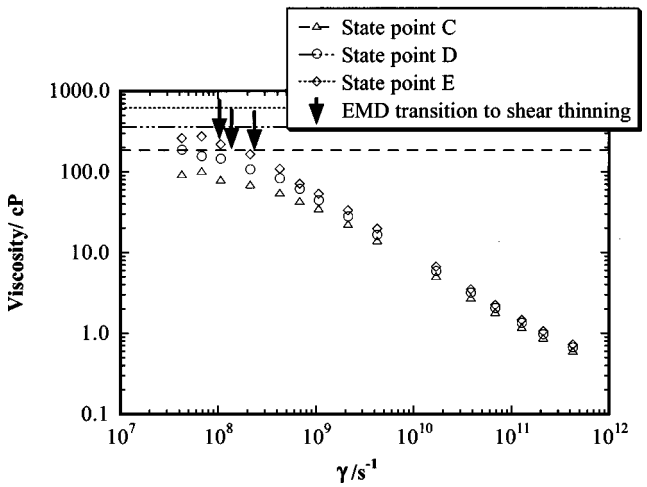

FIG. 2. Viscosity as a function of strain rate at state points C, D, and E from Table III.

TABLE VI. Viscosity versus strain rate data for 9-octylheptadecane at 372 K.

Strain rate/ s^{-1}	State point C		State point D		State point E	
	Run time/ns	Viscosity/ cP	Run time/ns	Viscosity/ cP	Run time/ns	Viscosity/ cP
4.24×10^{11}	3.07	0.6137	8.35	0.6756	7.45	0.7291
2.12×10^{11}	6.58	0.8859	7.55	0.9848	6.02	1.070
1.27×10^{11}	5.99	1.2045	7.60	1.352	6.39	1.479
6.78×10^{10}	4.81	1.832	7.31	2.091	5.00	2.267
3.82×10^{10}	7.60	2.787	5.83	3.201	7.45	3.566
1.70×10^{10}	10.5	5.133	8.02	6.059	7.80	6.730
4.24×10^{9}	15.7	14.23	5.45	16.79	13.4	19.85
2.12×10^{9}	15.0	22.66	5.47	28.50	17.9	33.68
1.06×10^{9}	18.2	35.29	25.3	45.05	17.6	53.98
6.78×10^{8}	20.5	43.87	25.5	62.15	19.4	71.50
4.24×10^{8}	18.4	55.46	30.0	83.93	13.4	110.1
2.12×10^{8}	36.6	70.34	22.2	107.7	37.3	166.2
1.06×10^{8}	38.6	80.34	33.6	147.2	45.9	221.7
6.78×10^{7}	68.8	103.1	67.0	157.8	69.3	276.9
4.24×10^{7}	62.2	94.27	65.6	189.7	66.4	263.4

times can be found in Table VI. In all cases the viscosity shows shear-thinning behavior at high strain rates, which levels off to a Newtonian plateau at lower strain rates. Again this transition to the Newtonian regime correlates well with the inverse of the rotational relaxation time. From the figure we see the transition to Newtonian behavior occurs at a lower strain rate for the less dense system and moves to higher strain rates with increasing density, meaning at higher pressures 9-octlyheptadecane first shows shear thinning behavior at lower strain rates. The Newtonian viscosity is higher at the highest density, though in the shear-thinning region the viscosity is virtually indistinguishable for the three state points.

The zero-shear viscosity can be estimated from the NEMD simulation data by averaging the values at strain rates that appear to fall within the Newtonian plateau. The NEMD predictions for all state points examined are given in Table VII along with the experimental value for comparison.[5,6] We see from the table that the united atom model underpredicts the zero-shear viscosity, though we note this UA model was parametrized for vapor–liquid equilibria and not transport properties. Since the zero-shear viscosity of 9-octylheptadecane is below 2 cSt at 100 °C (373 K) we were unable to determine the VI from the simulation results. Instead, we have calculated the VN, obtaining a value of 91, which compares very well with the experimental value of 94.[6,26]

Finally, the pressure–viscosity coefficient has been determined at 373 K from the NEMD simulation result for the zero-shear viscosity at each state point. Using the Barus re-

TABLE VII. Newtonian viscosity from NEMD simulations and experiment.

State point	A	B	C	D	E
η_{NEMD}/cP	4.40(±0.07)	1.36(±0.05)	87(±12)	165(±18)	270(±6.7)
$\eta_{EXPT.}$/cP	7.04[a]	1.86[a]	186[b]	358[b]	621[b]

[a]Taken from Ref. 6.
[b]Taken from Ref. 5.

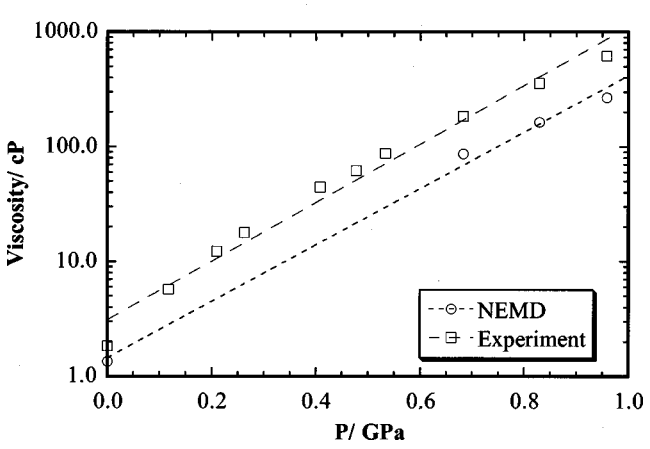

FIG. 3. Semilog plot of the viscosity as a function of pressure for 9-octylheptadecane.

lation and a semilog plot of the viscosity versus pressure at constant temperature, as given in Fig. 3, we can easily determine α. Experimentally for 9-octylheptadecane we obtain a value for α of 5.88 GPa^{-1} and from the NEMD simulation results a value of $5.66(\pm 0.04)$ GPa^{-1}, which is in very good agreement.

CONCLUSIONS

We have presented the results of EMD and NEMD simulations for 9-octylheptadecane at 311 and 372 K and pressures ranging from atmospheric to the gigapsacal range. The rotational relaxation time was determined from EMD simulations for each state point and found to be in good agreement with the predicted transition from Newtonian to non-Newtonian behavior from the NEMD simulation results. The zero-shear viscosity was estimated from the NEMD simulations and is seen to underpredict the experimental value, which is consistent with previous studies. From the zero-shear viscosity at atmospheric pressure and 372 and 311 K we determined the viscosity number for 9-octylhepadecane. The predicted value was found to be in excellent agreement with the experimental result. We also determined the pressure–viscosity coefficient using the empirical relation defined by Barus to describe the pressure dependence of the viscosity and achieved excellent agreement with the experimental result.

In earlier work we have extensively examined the influence of temperature on viscosity,[16,19,26] observing that while the united atom model underpredicts the actual viscosity of these molecules, it does correctly describe the temperature dependence. This work provides further support for that observation. Additionally, by examining the influence of pressure on viscosity we are able to conclude that the model appears to capture relative changes in viscosity with pressure as well as temperature. With this in mind molecular simulation could prove an invaluable tool when used to probe the rheological properties of as yet unsynthesized molecules, such as synthetic lubricant candidates. As advances in machine design lead to more demanding operating conditions, the performance advantages of synthetic lubricants with tailored molecular structure will become increasingly attractive.

ACKNOWLEDGMENTS

This work was supported in part by the Division of Materials Sciences of the U.S. Department of Energy. Oak Ridge National Laboratory is operated for the Department of Energy by Lockheed Martin Energy Research Corp. under Contract No. DE-AC05-96OR22464. Additional funding was provided by ExxonMobil Research and Engineering.

[1] E. W. Dean and G. H. B. Davis, Chem. Metall. Eng. **36**, 618 (1929).
[2] M. Sanchez-Rubio, A. Heredia-Veloz, J. E. Puig, and S. Gonzalez-Lozano, Lubr. Eng. **48**, 821 (1992).
[3] S. Bair, Tribol. Trans. **43**, 91 (2000).
[4] C. Barus, Am. J. Sci. **45**, 87 (1893).
[5] ASME Research Committee on Lubrication, New York, 1953.
[6] American Petroleum Institute, New York, 1966.
[7] R. Edberg, G. P. Morris, and D. J. Evans, J. Chem. Phys. **86**, 4555 (1987).
[8] G. P. Morris, J. Chem. Phys. **94**, 7420 (1991).
[9] A. Berker, S. Chynoweth, U. C. Klomp, and Y. Michopoulos, J. Chem. Soc., Faraday Trans. **88**, 1719 (1992).
[10] S. T. Cui, P. T. Cummings, and H. D. Cochran, J. Chem. Phys. **104**, 255 (1996).
[11] C. J. Mundy, J. I. Siepmann, and M. L. Klein, J. Chem. Phys. **102**, 3376 (1994).
[12] K. P. Travis and D. J. Evans, Mol. Simul. **17**, 157 (1996).
[13] S. T. Cui, S. A. Gupta, and P. T. Cummings, J. Chem. Phys. **105**, 1214 (1996).
[14] C. J. Mundy, S. Balasubramanian, K. Bagchi, J. I. Siepmann, and M. L. Klein, Faraday Discuss. **104**, 17 (1996).
[15] R. Khare, J. de Pablo, and A. Yethiraj, J. Chem. Phys. **107**, 6956 (1997).
[16] J. D. Moore, S. T. Cui, P. T. Cummings, and H. D. Cochran, AIChE J. **43**, 3260 (1997).
[17] M. Lahtela, M. Linnolahti, T. A. Pakkanen, and R. Rowley, J. Chem. Phys. **108**, 2626 (1998).
[18] L. I. Kioupis and E. J. Maginn, J. Phys. Chem. B **103**, 10 781 (1999).
[19] J. D. Moore, S. T. Cui, H. D. Cochran, and P. T. Cummings, J. Chem. Phys. **113**, 8833 (2000).
[20] J. I. Siepmann, S. Karaborni, and B. Smit, Nature (London) **365**, 330 (1993).
[21] B. Smit, S. Karaborni, and J . I . Siepmann, J. Chem. Phys. **102**, 2126 (1995).
[22] M. Mondello and G. S. Grest, J. Chem. Phys. **103**, 7156 (1995).
[23] M. E. Tuckerman, B. J. Berne, and G. J. Martyna, J. Chem. Phys. **97**, 1990 (1992).
[24] S. T. Cui, P. T. Cummings, and H. D. Cochran, J. Chem. Phys. **104**, 255 (1996).
[25] D. J. Evans and G. P. Morriss, *Statistical Mechanics of Nonequilibrium Liquids* (Academic, London, 1990).
[26] C. McCabe, S. T. Cui, and P. T. Cummings, Fluid Phase Equilibria (in press).